Hydrothermal vent complexes offshore Northeast Greenland: a potential role in driving the PETM

P. Reynolds[1, 2*], S. Planke[2, 3], J. M. Millett[2, 5], D. A. Jerram[3, 4], M. Trulsvik[2], N. Schofield[5], R. Myklebust[6]

[1] Centre for Tectonics, Resources and Exploration (TRaX), Australian School of Petroleum, University of Adelaide, Adelaide, SA 5005, Australia

[2]Volcanic Basin Petroleum Research (VBPR), Oslo Science Park, Norway

[3]Centre for Earth Evolution and Dynamics (CEED), University of Oslo, Norway

[4]DougalEARTH Ltd., Solihull, UK

[5]Department of Geology and Petroleum Geology, University of Aberdeen, UK

[6]TGS, Lensmannslia 4, 1386 Asker, Norway

*Corresponding author: peter.reynolds@adelaide.edu.au, +61484607355

ABSTRACT

Continental rifting is often associated with voluminous magmatism and perturbations in the Earth's climate. In this study, we use 2D seismic data from the northeast Greenland margin to document two Paleogene-aged sill complexes ≥18 000 and ≥10 000 km^2 in size. Intrusion of the sills resulted in the contact metamorphism of carbon-rich shales, producing thermogenic methane which was released via 52 newly discovered hydrothermal vent complexes, some of which reach up to 11 km in diameter. Mass balance calculations indicate that the volume of methane produced by these intrusive complexes is comparable to that required to have caused the negative $\delta^{13}C$ isotope excursion associated with the PETM. Combined with data from the conjugate Norwegian margin, our study provides evidence for margin-scale, volcanically-

induced greenhouse gas release during the late Paleocene/early Eocene. Given the abundance of similar-aged sill complexes in Upper Paleozoic-Mesozoic and Cretaceous-Tertiary basins elsewhere along the northeast Atlantic continental margin, our findings support a major role for volcanism in driving global climate change.

Keywords

Hydrothermal vent complexes, sill intrusions, PETM, global climate change, Greenland, NAIP

1. Introduction

Volcanic rifted margins are associated with voluminous extrusive and intrusive igneous activity (Menzies et al., 2002; Jerram and Widdowson, 2005) of which the northeast Atlantic margins are type examples (e.g. Saunders et al., 1997). Here, extrusive activity during the Paleocene and Eocene produced characteristic Seaward Dipping Reflectors and extensive subaerial lava flows, whilst intrusive activity produced igneous centres (Jerram and Bryan, 2015) and sill complexes ≥80 000 km^2 in size (Planke et al., 2005; Schofield et al. 2015).

The emplacement of sill complexes can generate huge quantities of greenhouse gases by metamorphic reactions within the intrusion aureole system (e.g. Aarnes et al., 2011, 2012, 2015). The composition and volumes of gases generated are dependent on a range of factors including (and most importantly) host rock composition, total organic content (TOC) and permeability; in addition to intrusion volume, temperature and emplacement depth (Aarnes et al., 2012; Iyer et al., 2013). A proportion of these gases are released to the atmosphere or hydrosphere through hydrothermal vent complexes within tens of years of sill intrusion (e.g. Jamtveit et al., 2004; Aarnes et al., 2010). Hydrothermal vent complexes commonly form above sill tip terminations as a result of intensive fracturing or brecciation of overburden strata in the shallow subsurface. These overburden breaches are caused by overpressure build up

associated with the boiling of pore fluids and host rock devolatilization reactions (Jamtveit et al., 2004; Aarnes et al., 2012). Where vent structures are observed in seismic data, they have eye, dome or crater-like upper parts (Planke et al., 2005; Møller Hansen, 2006). The lower parts are characterised by a central pipe, commonly surrounded by a region of inwardly dipping strata that is contained within metamorphosed sedimentary rocks (Møller Hansen, 2006; Svensen et al., 2007). Release of gases from these vents is thought to have played a primary role in driving global warming, as proposed for the Paleocene Eocene Thermal Maximum (PETM) (Svensen et al., 2004).

Extensive sill complexes are documented from the United Kingdom Continental Shelf (e.g. Schofield et al., 2015) and the Norwegian margin (Svensen et al., 2004) where hydrothermal vent complexes are also recognised. Whilst onshore studies have documented sills within Carboniferous−Cretaceous-aged sediments (Price et al., 1997; Therkelsen, 2016), sparse data coverage in regions covered by sea ice and poor seismic imaging beneath the “top basalt” reflection means that the offshore section of this margin has long been a significant gap in our understanding of the northeast Atlantic continental margins. Without the full extent of intrusive complexes in the North Atlantic Igneous Province (NAIP) being recognised and mapped, the role of margin-scale intrusive volcanic activity in driving global climate change has remained uncertain.

This study uses newly acquired 2D seismic data to document the distribution and architecture of sill complexes and associated hydrothermal vent complexes along the offshore northeast Greenland margin. A combination of seismic mapping, field evidence (e.g. Larsen and Marcussen, 1992) and burial history curves (Mathiesen et al., 2000) indicate that the sills within the Danmarkshavn Basin regionally intruded Jurassic-aged, shale-rich horizons at paleodepths of >3 km, whilst in the Thetis Basin they intruded Cretaceous-aged host rocks at paleodepths of 1−2 km. The Jurassic-aged shales have TOC (total organic carbon) contents up

to twenty times higher than those reported from the Norwegian margin (Svensen et al., 2004; Price and Whitham 1997). Contact metamorphism of these shales resulted in the voluminous production of greenhouse gases such as methane, released into to the atmosphere via hydrothermal vent complexes (Svensen et al., 2004; Aarnes et al., 2015). Combined with data from the Norwegian and United Kingdom Continental Shelf margins, we show that volcanically-induced greenhouse gases were produced on a scale capable of producing the observed negative $\delta^{13}C$ excursion during the PETM.

2. Dataset and Methods

This study utilizes 2D seismic profiles acquired by TGS in 2008−9 and 2011−14, including re-processed AWI data. The surveys cover an area of ~125 000 km^2, with the lines ranging from 40−250 km in length and spacings varying from 0.1−40 km. Seismic interpretation was conducted using Kingdom software. The extrusive and intrusive volcanic facies have been mapped on intersecting 2D seismic lines (Fig. 1) using the seismic volcanostratigraphic methods of Planke et al. (2000) and Planke et al. (2015). In the absence of well data we use a p-wave velocity of 5.5 km s^{-1} to determine the resolution and detection limit for the sills (Skogly, 1998; Berndt et al., 2000) and a velocity of 1.8 km s^{-1} to calculate the dimensions of the upper parts of the vents (Planke et al., 2005). The sedimentary basins are correlated with the onshore successions of east and northeastern Greenland, and offshore successions in the southern Barents Sea and on the mid-Norwegian shelf (Hamann et al., 2005; Tsikalas et al., 2005). More than one hundred gravity core and tens of dredges have been acquired to study hydrocarbon seepages and to allow seismostratigraphic ties.

3. Interpretation of sill and hydrothermal vent complexes

100 The sills are characterised by high amplitude, positive reflections, indicating a significant
101 downwards increase in acoustic impedance. They commonly display abrupt terminations,
102 saucer shaped morphologies and transgress the stratigraphy (Figs. 2 and 3); diagnostic features
103 of igneous intrusions (e.g. Planke et al., 2005; 2015). The sills are dominantly found within
104 two complexes; a ≥18 000 km^2 complex in the Cretaceous-Tertiary age Thetis Basin and a ≥10
105 000 km^2 complex in the Upper Paleozoic-Mesozoic-aged Danmarkshavn Basin. The sills
106 within these complexes are also documented by Hamann et al., (2005) and Geissler et al.,
107 (2016). The sill complexes follow the structural trend of the basins and are oriented NNE/SSW
108 (Fig. 2). Within the Thetis Basin the sills are up to 28 km in diameter and were emplaced at
109 depths of 1−2 km; this is interpreted from their relationship to the Vent Horizon (see below).
110 In the Danmarkshavn Basin the sills are up to 40 km in diameter and were emplaced at depths
111 of 3−5 km. The sills in the Danmarkshavn Basin tend to be more layer parallel than those in
112 the Thetis Basin, which are commonly saucer-shaped (Fig. 2). This morphological-depth
113 relationship is typical of sill complexes (Planke et al., 2015).
114 Sills are not imaged beneath the extrusive facies (e.g. Inner Flows; see Planke et al., 2000)
115 and are absent within the Danmarkshavn Ridge. Sparse data coverage prevents us from
116 determining the northward extent of the complex in the Thetis Basin. The frequency of the
117 seismic data at the depths at which the sills are found is 10 Hz, therefore the sills need to be
118 >200 m thick to be resolved and >50 m thick to be detected. Although imaging of deep sills
119 and distinguishing sills from multiples beneath the first high amplitude sill reflection event is
120 challenging, intersecting seismic surveys indicate that the sills are vertically stacked, with each
121 complex containing ≥4 sills which decrease in number toward the basin margins.
122 Linked to the tips of the sills by vertical chimney zones of disturbed reflections are a series
123 of hydrothermal vent complexes. These vents have eye-, dome- and crater-type upper parts,
124 similar to those on the conjugate Norwegian margin (Planke et al., 2005). The eye- and dome-

type vents have sub-parallel, prograding internal reflections whilst the crater-type vents have internal reflections which vary from chaotic to parallel. We calculate the upper part of the vent complexes are 36−504 m in height. The diameter of the vents ranges from 0.7−11 km (e.g. Fig. 4). Within the Thetis Basin, the upper parts of all vents are located at a consistent stratigraphic horizon which is onlapped by overlying reflections; this is identified as the Vent Horizon (VH). Onlap relationships indicate the VH represents the paleosurface at the time of sill intrusion. Within the Danmarkshavn Basin, the VH forms the top of the crater-type vents. Towards the Volcanic Complex, the VH terminates against the Inner Flows (Fig. 5).

A total of 52 vent complexes have been identified from both the Danmarkshavn (n=17) and Thetis basins (n=35). However, it is likely there are many more hydrothermal vents which are not intersected by the available 2D seismic lines. The vents have previously been documented by Geissler et al., (2016) and are distinguished from superficially similar volcanoes by their stratigraphic position, lower amplitude and differing internal reflections (cf. Fig. 12 in Schofield et al., 2015 and Reynolds et al., 2016). The vents are distinguished from biogenic mounds since they are much smaller than these features and they do not form above faults (e.g. Langhi et al., 2016). Furthermore, the vents we describe are ubiquitously associated with sills (e.g. Figs. 3 and 6) typical of hydrothermal vents (e.g. Planke et al., 2005) and unlike other mounded structures (e.g. Hansen et al., 2005).

4. Determining the effects of thermogenic methane release

4.1 Host Rock Properties

The quantity of gas produced during contact metamorphism is greatly influenced by the host rock properties. In the Cretaceous-aged Thetis Basin, the sills are inferred to have been intruded at depths of 1−2 km into sedimentary rocks with TOC's ranging from 0.5−2%; as observed along the conjugate Møre and Vøring basins (Svensen et al., 2004; Aarnes et al.,

2015). Conversely, our observations from seismic data in the Upper Paleozoic Danmarkshavn Basin indicate the sills were emplaced at depths >3 km. This observation is supported by field and apatite-fission track data from the Upper Paleozoic-Mesozoic-aged basins of east Greenland, which indicate the sills are intruded at depths of >3 km into Jurassic-aged shales (Larsen and Marcussen, 1992). These shales have TOC contents ranging from 4−10% (Price and Whitham 1997), suggesting that the quantities of gas produced during contact metamorphism in the Danmarkshavn Basin were significantly higher than in Cretaceous and Paleocene basins elsewhere on the northeast Atlantic continental margin.

4.2 Quantities of gas produced

Following the method of Svensen et al. (2004), we calculate that the mass of methane (W_{CH4}) produced during contact metamorphism is: $W_{CH4} = 1.34 F_C V_A \rho$, where 1.34 is the atomic weight conversion factor between carbon and methane, F_C is equal to the TOC content of the host rock, V_A is the volume of the aureole and ρ is rock density (2400 kg m^{-3}). In our calculations we assume TOC contents of 4−10 wt. % in the Danmarkshavn Basin and 0.5−2 wt.% in the Thetis Basin. To calculate V_A we assume an aureole thickness of 100−600 m. This is based on our seismic data which indicates the sills are >>50 m thick, and the observation that aureole thickness for sills >50 m thick is equal to one sill thickness above and below the intrusion (Svensen et al., 2004). This sill to aureole thickness relationship is supported by many field and borehole studies globally (see review by Aarnes et al., 2010) and is supported by the closest analogue to the study area, where similar-aged intrusions of the Utgard sill complex were penetrated by well 6607/5-2 in the Vøring Basin (Aarnes et al., 2015). In the Utgard case, a ~1 km thick stratigraphic interval was demonstrated to be effected by the near simultaneous emplacement of two c. 100 m thick sills. Field data from east Greenland also supports our

interpretation, where sills typically range in thickness from 50−300 m (Larsen and Marcussen, 1992; Planke et al., 2005).

Based on these assumptions, our calculations indicate 0.06−1.73 × 10^{18} g of methane was produced from the Danmarkshavn Basin and an additional 0.01−0.62 × 10^{18} g of methane would have been produced as a result of intrusion emplacement in the Thetis Basin. The combined range for gas production along the northeast Greenland margin therefore equals 0.07−2.36× 10^{18} g of methane. These values represent 50−90% of the total gas production potential of the source rocks, since gas production depends on kerogen type (Hunt, 1996). Lower volumes of thermogenic gas may be produced during contact metamorphism as a result of heating of sediment pore water and trapping of volatiles (e.g. Gröcke et al., 2009). Gas volume production also varies as a result of host rock permeability, background temperature, aureole thermal profile and heat transfer mechanism (Aarnes et al., 2010; Iyer et al., 2013). However, we highlight that the main controls on the volume of gas produced are host rock composition, TOC, sill thickness and sill extent (Aarnes et al., 2011; Iyer et al., 2013) which we have accounted for in our estimates.

Additionally, there are several reasons for which we suggest that our estimate of gas production represents a conservative estimate. Firstly, many sills may be below the resolution of the seismic data (Schofield et al., 2015). Secondly, the calculated volumes do not include the poorly imaged regions beneath areas covered by extrusive volcanic rocks and areas with limited data coverage due to sea ice. Thirdly, the formation of hydrothermal vent complexes may have resulted in the breaching of pre-existing hydrocarbon reservoirs (e.g. Price & Whitham, 1997; Svensen et al., 2004) further adding to the potential quantities of gas released. Finally, our estimates do not include the contribution of magmatic CO_2 produced from degassing of the intrusions. It has been proposed that at the margin scale, volcanic CO_2 emissions are capable of complementing thermogenic gas release in perturbing the Earths'

atmosphere (Eldholm & Thomas, 1993; Saunders, 2016). Assessing the quantitative volumes of CO_2 released by intrusions is challenging without constraints on the volatile contents of the magmas emplaced into the Danmarkshavn and Thetis basins, however, such contributions could have increased the overall volume of released greenhouse gases supporting the conservative nature of our estimates.

4.3 Effect of gas release on the Paleocene carbon reservoir

To determine the potential climatic impact of thermogenic gas release, it is important to constrain the isotopic mass balance of the Paleocene carbon reservoir. To do this, we use the method described by Mc Inerney and Wing (2011). We assume that the initial mass of the Paleocene surface reservoir was 50×10^{18} g C, its carbon isotope ratio was −2.5‰ and that thermogenic methane has a $\delta^{13}C$ of ~−30‰ (McInerney and Wing, 2011). We also use a value of −3.5‰ for the PETM initial isotope excursion in $\delta^{13}C$ (Zachos et al., 2007; Sluijs and Dickens, 2012). Based on these assumptions, we estimate that 2.5×10^{18} g CH_4 would have been required to cause the negative $\delta^{13}C$ excursion during the PETM. Our conservative estimates of gas production indicate that a comparable volume (2.36×10^{18} g) could have been produced along the northeast Greenland margin. A large proportion of these gases may have reached the atmosphere regardless of whether or not the eruptions occurred in the marine environment; numerical modelling shows that methane plumes formed during subaqueous gas eruptions do not become fully dissolved or oxidised in the ocean (Zhang, 2003).

5. Discussion

The absence of well data from the hydrothermal vents on the northeast Greenland margin prevents us from attaining the 10−100's ka resolution required to directly link vent formation to the PETM. Additionally, Iyer et al. (in review) document that not all generated gases will be

outgassed to the atmosphere within the short timescales associated with climate perturbations. However, the VH gives a robust relative time datum which is unequivocally associated with active venting across the northeast Greenland margin. This reflection can be clearly mapped laterally from the Thetis Basin to the SE where it terminates against the Inner Flows facies. A similar temporal relationship is observed for vent complexes on the Norwegian margin where the TV horizon, which represents the upper part of the vent complexes, terminates against the Inner Flows (Planke et al., 2005). Igneous intrusions, associated venting and the eruption of the Inner Flows on the Norwegian margin occurred during the onset of continental breakup at c. 55.6 Ma (Planke et al., 2005; Svensen et al., 2010). Given the conjugate nature of the two margins and the well-documented temporal and spatial association of the Inner Flows volcanism with continental break-up (Planke et al., 2000) it is highly likely that both the Inner Flows and venting occurred at similar times on either side of the developing rift system near the Paleocene-Eocene boundary. Our interpretation that venting occurred at this time is supported by radiometric dating of onshore volcanic rocks along the northeast Greenland margin which indicates that the main phase of volcanism occurred at 56−53 Ma (Larsen et al., 2014). Since hydrothermal vent complexes form within tens of years of sill intrusion (e.g. Jamtveit et al., 2004; Aarnes et al., 2010) the complexes identified within this study formed in close temporal proximity to the PETM which occurred at ~55.5 Ma (Westerhold et al., 2009).

We also note that along the Norwegian margin, an additional $0.3{-}3.0 \times 10^{18}$ g of methane was produced as a result of sill emplacement (Svensen et al., 2004). Combined with the contribution from the northeast Greenland margin, this creates a combined volume of $0.37{-}5.5 \times 10^{18}$ g of methane produced by sill emplacement (Fig. 7). Additional sill complexes emplaced prior to the PETM are also briefly documented along the eastern Greenland margin (Larsen and Marcussen, 1992) and have been extensively mapped within the Faroe-Shetland Basin (Schofield et al., 2015). As detailed in this study, these sills were intruded into both Upper

Paleozoic-Mesozoic and Cretaceous-Tertiary basins (Larsen and Marcussen, 1992; Schofield et al., 2015). Given the ubiquity of hydrothermal vent complexes now identified along the Norwegian and northeast Greenland margins, it is likely that the total volume of thermogenic methane produced during intrusion-induced metamorphism could have easily produced the negative $\delta^{13}C$ excursion observed during the PETM.

6. Summary

Continental rifting is commonly associated with voluminous magmatism and perturbations in the Earth's climate. Our study uses newly acquired seismic data from the northeast Greenland margin to reveal the extent of two previously unconstrained offshore sill complexes emplaced during rifting of the Northeast Atlantic continental margin. Intrusion emplacement into shale-dominated sedimentary rocks with TOC contents of up to 10% resulted in rapid contact metamorphism and the production of up to 2.36×10^{18} g of methane. Much of this methane was released within tens of years of sill intrusion via a series of newly-discovered hydrothermal vent complexes. These vent complexes present the first evidence for thermogenic methane release along the northeast Greenland margin. The volume of gas produced along this margin alone is approaching that capable of causing the negative $\delta^{13}C$ excursion observed during the PETM. Combined with the volume of methane released from similar vents in the Vøring and Møre basins, and the ubiquity of similar-aged sill complexes elsewhere along the Norwegian and UK margins, we suggest that volcanically-induced greenhouse gas release was a common and important phenomenon along the northeast Atlantic margins in close proximity to the PETM. This study highlights and supports the important role of volcanic activity in driving global-scale climate change.

References

Aarnes, I., Svensen, H., Connolly, J. a. D., and Podladchikov, Y.Y., 2010, How contact metamorphism can trigger global climate changes: Modeling gas generation around igneous sills in sedimentary basins: Geochimica et Cosmochimica Acta, v. 74, no. 24, p. 7179–7195, doi: 10.1016/j.gca.2010.09.011.

Aarnes, I., Fristad, K., Planke, S., and Svensen, H., 2011, The impact of host-rock composition on devolatilization of sedimentary rocks during contact metamorphism around mafic sheet intrusions: Geochemistry, Geophysics, Geosystems, v. 12, no. 10.

Aarnes, I., Podladchikov, Y., and Svensen, H., 2012, Devolatilization-induced pressure build-up: Implications for reaction front movement and breccia pipe formation: Geofluids, v. 12, no. 4, p. 265–279, doi: 10.1111/j.1468-8123.2012.00368.x.

Aarnes, I., Planke, S., Trulsvik, M., and Svensen, H., 2015, Contact metamorphism and thermogenic gas generation in the Vøring and Møre basins, offshore Norway, during the Paleocene–Eocene thermal maximum: Journal of the Geological Society, v. 172, no. 5, p. 588–598, doi: 10.1144/jgs2014-098.

Aubourg, C., Techer, I., Geoffroy, L., Clauer, N., and Baudin, F., 2014, Detecting the thermal aureole of a magmatic intrusion in immature to mature sediments: a case study in the East Greenland Basin (73°N): Geophysical Journal International, v. 196, no. 1, p. 160-174.

Berndt, C., Skogly, O., Planke, S., Eldholm, O., and Mjelde, R., 2000, High-velocity breakup-related sills in the Voring Basin, off Norway: Journal of Geophysical Research, v. 105, no. B12, p. 28443-28428,28454.

Chalmers, J.A., Larsen, L.M., and Pedersen, A.K., 2013, Widespread Palaeocene volcanism around the northern North Atlantic and Labrador Sea : evidence for a large, hot, early plume head, Journal of the Geological Society, v. 152, no. 6, p. 965-969

298 Dunkley Jones, T., D. J. Lunt, D. N. Schmidt, A. Ridgwell, A. Sluijs, P. J. Valdes, and M.
299 Maslin, 2013, Climate model and proxy data constraints on ocean warming across the
300 Paleocene-Eocene Thermal Maximum, Earth Sci. Rev., 125, 123–145.
301 Eldholm, O., and Thomas, E., 1993, Environmental impact of volcanic margin formation: Earth
302 and Planetary Science Letters, v. 117, p. 319-329.
303 Geissler, W. H., Gaina, C., Hopper, J. R., Funck, T., Blischke, A., Arting, U., Horni, J. Á.,
304 Péron-Pinvidic, G., and Abdelmalak, M. M., 2016, Seismic volcanostratigraphy of the
305 NE Greenland continental margin: Geological Society, London, Special Publications, v.
306 447, p. SP447. 411.
307 Gröcke, D. R., Rimmer, S. M., Yoksoulian, L. E., Cairncross, B., Tsikos, H., and van Hunen,
308 J., 2009, No evidence for thermogenic methane release in coal from the Karoo-Ferrar
309 large igneous province: Earth and Planetary Science Letters, v. 277, no. 1–2, p. 204-212.
310 Hald, N., and Tegner, C., 2000, Composition and age of tertiary sills and dykes, Jameson Land
311 Basin, East Greenland: relation to regional flood volcanism: Lithos, v. 54, no. 3–4, p.
312 207-233.
313 Hamann, N.N., Whittaker, R.C., Stermmerik., L 2005, Geological development of the
314 Northeast Greenland Shelf. Geological Society, London, Petroleum Geology
315 Conference series, v. 6, p.887-902
316 Hansen, J., Cartwright, J., Huuse, M., and Clausen, O. R., 2005, 3D seismic expression of fluid
317 migration and mud remobilization on the Gjallar Ridge, offshore mid-Norway: Basin
318 Research, v. 17, no. 1, p. 123-139.
319 Hunt, J., 1996, Petroleum geology and geochemistry, New York, Freeman and Company.
320 Iyer, K., Rüpke, L., and Galerne, C.Y., 2013, Modeling fluid flow in sedimentary basins with
321 sill intrusions: Implications for hydrothermal venting and climate change:

322 Geochemistry, Geophysics, Geosystems, v. 14, no. 12, p. 5244–5262, doi:
323 10.1002/2013GC005012.
324 Jamtveit, B., Svensen, H., Podladchikov, Y. Y., and Planke, S., 2004, Hydrothermal vent
325 complexes associated with sill intrusions in sedimentary basins: Physical geology of
326 high-level magmatic systems, v. 234, p. 233-241.
327 Jerram, D. A., Widdowson, M., 2005. The anatomy of Continental Flood Basalt Provinces:
328 geological constraints on the processes and products of flood volcanism. Lithos 79,
329 385-405.
330 Jerram, D.A., Bryan., S.E., 2015. Plumbing Systems of Shallow Level Intrusive Complexes.
331 Advances in Volcanology, Springer Berlin Heidelberg
332 Langhi, L., Strand, J., and Ross, A. S., 2016, Fault-related biogenic mounds in the Ceduna Sub-
333 basin, Australia. Implications for hydrocarbon migration: Marine and Petroleum
334 Geology, v. 74, p. 47-58.
335 Larsen, H. C., and Marcussen, C., 1992, Sill-intrusion, flood basalt emplacement and deep
336 crustal structure of the Scoresby Sund region, East Greenland: Geological Society,
337 London, Special Publications, v. 68, no. 1, p. 365-386.
338 Larsen, L.M., Pedersen, a. K., Tegner, C., and Duncan, R. a., 2014, Eocene to Miocene igneous
339 activity in NE Greenland: northward younging of magmatism along the East Greenland
340 margin Eocene to Miocene igneous activity in NE Greenland : northward younging of
341 magmatism along the East Greenland margin: Journal of the Geological Society, v. 171,
342 no. 4, p. 539–553.
343 Mathiesen A, Bidstrup T, Christiansen FG (2000) Denudation and uplift history of the Jameson
344 Land basin, East Greenland—constrained from maturity and apatite fission track data.
345 Global and Planetary Change, v. 24, no. 3, p.275−301.

McInerney, F. A., and Wing, S. L., 2011, The Paleocene-Eocene Thermal Maximum: a perturbation of carbon cycle, climate, and biosphere with implications for the future: Annual Review of Earth and Planetary Sciences, v. 39, p. 489-516.

Menzies, M.A., Klemperer, S.L., Ebinger, C.J., and Baker, J., 2002, Characteristics of volcanic rifted margins: Geological Society of America Special Paper, v. 362, p. 1–14.

Møller Hansen, D., 2006, The morphology of intrusion-related vent structures and their implications for constraining the timing of intrusive events along the NE Atlantic margin: Journal of the Geological Society, v. 163, no. 5, p. 789−800.

Planke, S., Symonds, P. A., Alvestad, E., and Skogseid, J., 2000, Seismic volcanostratigraphy of large-volume basaltic extrusive complexes on rifted margins: J. Geophys. Res., v. 105, no. B8, p. 19335-19351.

Planke, S., Rasmussen, T., Rey, S., and Myklebust, R., 2005, Seismic characteristics and distribution of volcanic intrusions and hydrothermal vent complexes in the Vøring and Møre basins, *in* Proceedings Geological Society, London, Petroleum Geology Conference series, Geological Society of London, v. 6, p. 833−844.

Planke, S., Svensen, H., Myklebust, R., Bannister, S., Manton, B., and Lorenz, L., 2015, Geophysics and Remote Sensing, *in* Advances in Volcanology, p.1−16, doi: 10.1007/11157-2014-6

Price, S., Brodie, J., Whitman, A., and Kent, R. A. Y., 1997, Mid-Tertiary rifting and magmatism in the Traill Ø region, East Greenland: Journal of the Geological Society, v. 154, no. 3, p. 419−434.

Price, S. P., and Whitham, A. G., 1997, Exhumed hydrocarbon traps in East Greenland: analogs for the Lower-Middle Jurassic play of Northwest Europe: AAPG bulletin, v. 81, no. 2, p. 196−221.

Reynolds, P., Schofield, N., Brown, R. J., and Holford, S., 2016, The architecture of submarine monogenetic volcanoes – insights from 3D seismic data: Basin Research, p. n/a-n/a.

Saunders, A.D., Fitton, J.G., Kerr, A.C., Norry, M.J., and Kent, R.W., 1997, The north Atlantic igneous province, *in* Mahoney, J.J. and Coffin, M.F. eds., Large Igneous Provinces: Continental, and Planetary Flood Volcanism, Geophysical Monograph 100, American Geophysical Union, p. 45–93.

Saunders, A. D., 2016, Two LIPs and two Earth-system crises: the impact of the North Atlantic Igneous Province and the Siberian Traps on the Earth-surface carbon cycle: Geological Magazine, v. 153, no. 2, p. 201-222.

Schofield, N., Holford, S., Millett, J. M., Brown, D., Jolley, D., R. Passey, S., Muirhead, D., Grove, C., Magee, C., Murray, J., Hole, M., A.-L. Jackson, C., and Stevenson, C., 2015, Regional magma plumbing and emplacement mechanisms of the Faroe-Shetland Sill Complex: implications for magma transport and petroleum systems within sedimentary basins: Basin Research, doi:10.1111/bre.12164.

Skogly, O., 1998, Seismic characterization and emplacement of intrusives in the Vøring Basin: Cand Scient thesis, Department of Geology, University of Oslo.

Sluijs, A., and Dickens, G. R., 2012, Assessing offsets between the δ13C of sedimentary components and the global exogenic carbon pool across early Paleogene carbon cycle perturbations: Global Biogeochemical Cycles, v. 26, no. 4.

Svensen, H., Planke, S., Chevallier, L., Malthe-Sørenssen, A., Corfu, F., and Jamtveit, B., 2007, Hydrothermal venting of greenhouse gases triggering Early Jurassic global warming: Earth and Planetary Science Letters, v. 256, no. 3–4, p. 554−566.

Svensen, H., Planke, S., and Corfu, F., 2010, Zircon dating ties NE Atlantic sill emplacement to initial Eocene global warming: Journal of the Geological Society, v. 167, no. 3, p. 433−436.

Svensen, H., Planke, S., Malthe-Sorenssen, A., Jamtveit, B., Myklebust, R., Rasmussen Eidem, T., and Rey, S. S., 2004, Release of methane from a volcanic basin as a mechanism for initial Eocene global warming: Nature, v. 429, no. 6991, p. 542−545.

Therkelsen, J., 2016, Diagenesis and reservoir properties of Middle Jurassic sandstones, Traill Ø, East Greenland: The influence of magmatism and faulting: Marine and Petroleum Geology, v. 78, p. 196-221.

Tsikalas, F., Faleide, J., Eldholm, O., and Wilson, J., 2005, Late Mesozoic–Cenozoic structural and stratigraphic correlations between the conjugate mid-Norway and NE Greenland continental margins, *in* Proceedings Geological Society, London, Petroleum Geology Conference series, Geological Society of London, v. 6, p. 785−801.

Westerhold, T., Röhl, U., McCarren, H. K., and Zachos, J. C., 2009, Latest on the absolute age of the Paleocene–Eocene Thermal Maximum (PETM): new insights from exact stratigraphic position of key ash layers+ 19 and− 17: Earth and Planetary Science Letters, v. 287, no. 3, p. 412-419.

Zachos, J. C., Bohaty, S. M., John, C. M., McCarren, H., Kelly, D. C., and Nielsen, T., 2007, The Palaeocene–Eocene carbon isotope excursion: constraints from individual shell planktonic foraminifer records: Philosophical Transactions of the Royal Society of London A: Mathematical, Physical and Engineering Sciences, v. 365, no. 1856, p. 1829-1842.

Zhang, Y., 2003, Methane escape from gas hydrate systems in marine environment, and methane-driven oceanic eruptions: Geophysical Research Letters, v. 30, no. 7.

Acknowledgements

TGS are thanked for access to data and Dwarika Maharjan is thanked for help with Kingdom software. Andy Saunders and Mads Huuse are thanked for insightful, constructive reviews and Tamsin Mather is thanked for editorial handling.

Figures

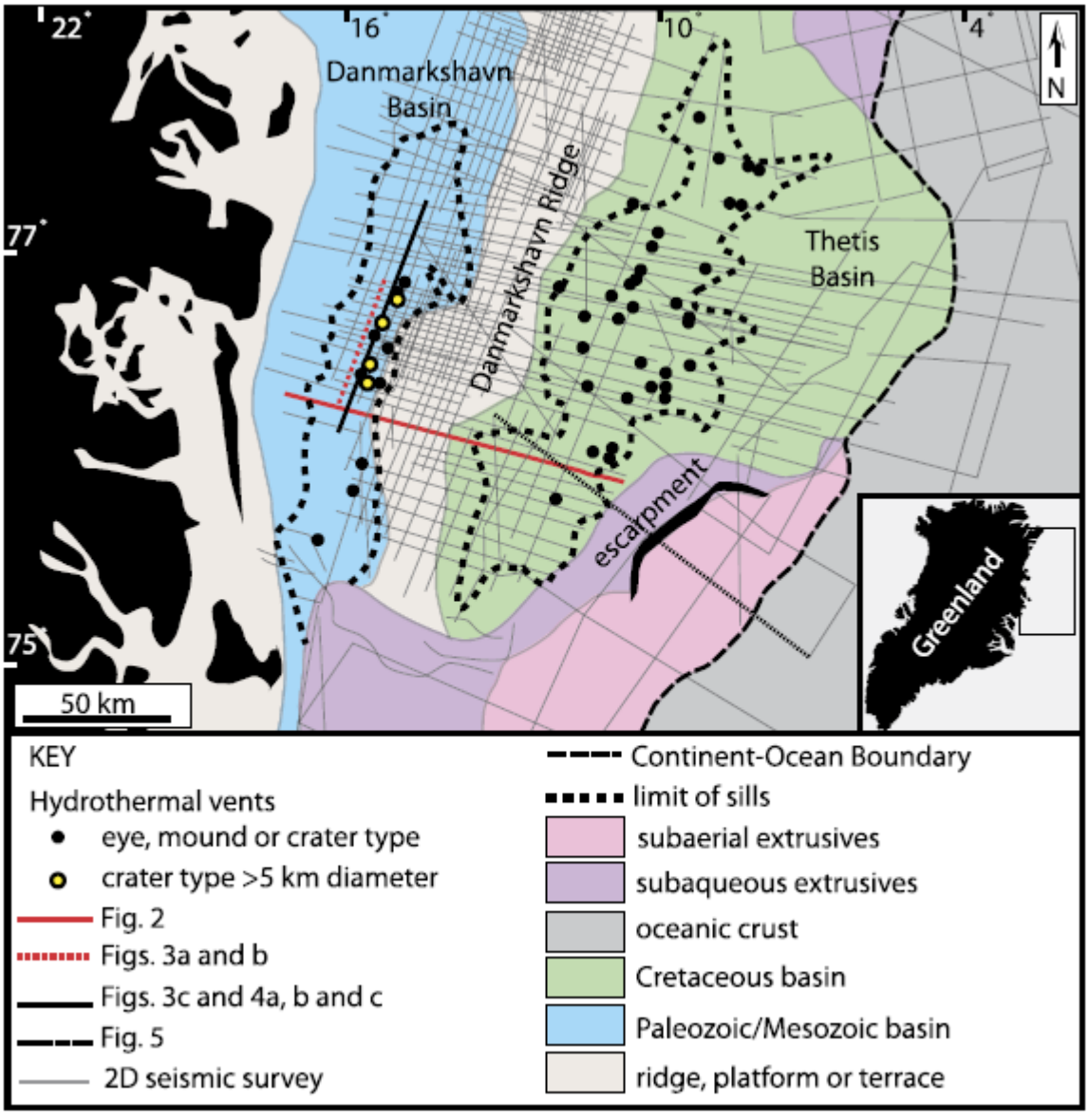

Figure 1. Map showing the Danmarkshavn and Thetis Basins and the distribution of volcanic units. Inset shows the location of the study area along the Greenland coast. Adapted from Hamann et al., 2005.

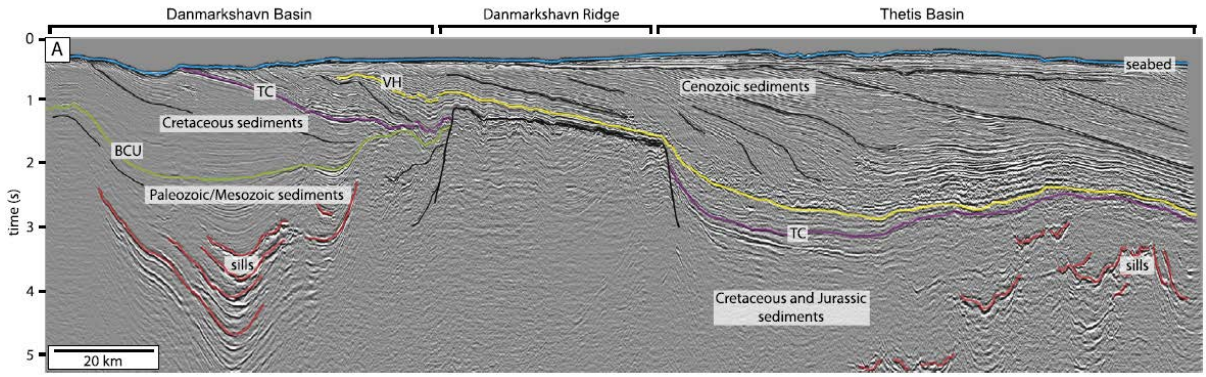

Figure 2. Seismic cross section showing sills within the Danmarkshavn and Thetis Basins. VH=Vent Horizon, TC=Top Cretaceous, BCU=Base Cretaceous Unconformity. Note that the sills in both basins are represented by white reflections, the same polarity as the seabed.

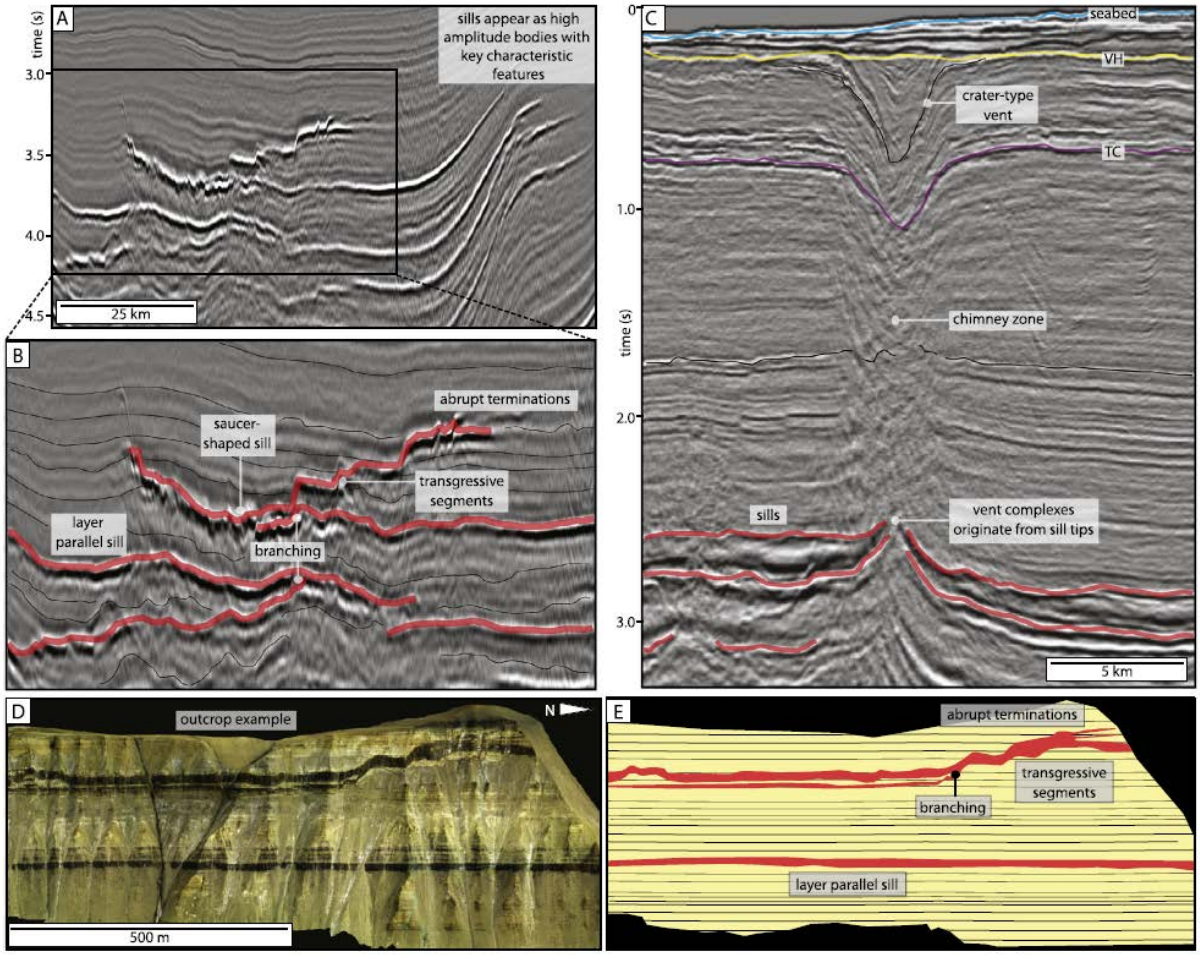

Figure 3. Diagram illustrating key features of sills. Images A and B are seismic cross sections of sills in the Danmarkshavn Basin. Note that the sills are high amplitude, positive reflections with layer parallel and saucer-shaped morphologies which transgress the stratigraphy. Image

C shows a crater-type vent linked to the tip of a sill within the Danmarkshavn Basin. See Figure 1 for location. Images D and E show field examples of sills from onshore Northeast Greenland with the same characteristics as the seismic examples.

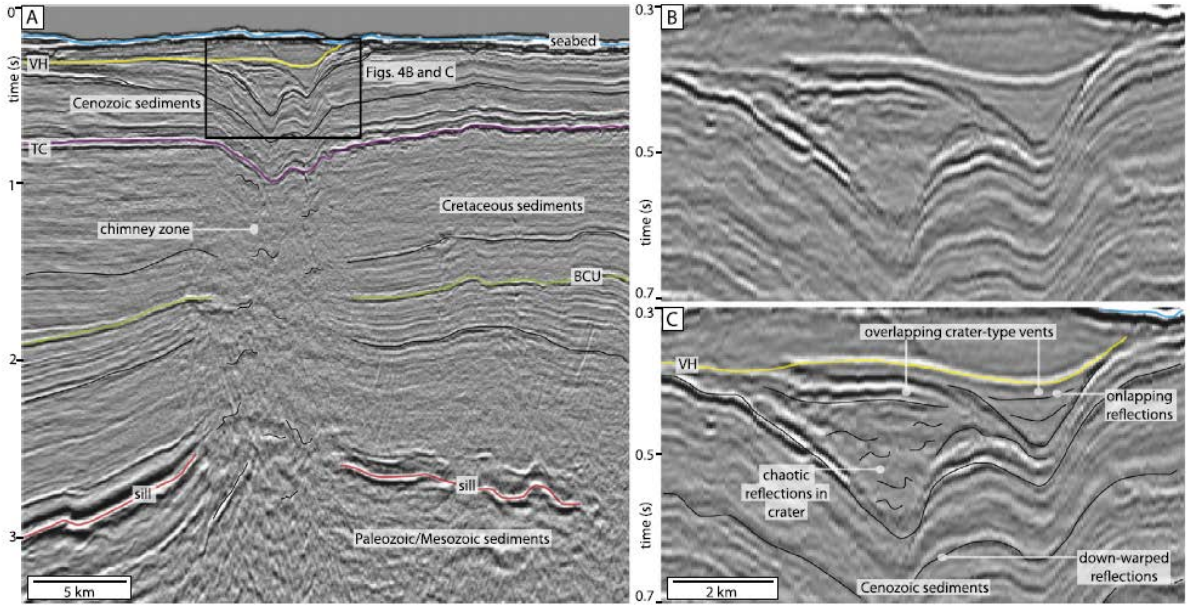

Figure 4. Seismic sections of crater-type hydrothermal vents above sills within the Danmarkshavn Basin. VH=Vent Horizon, TC=Top Cretaceous, BCU=Base Cretaceous Unconformity.

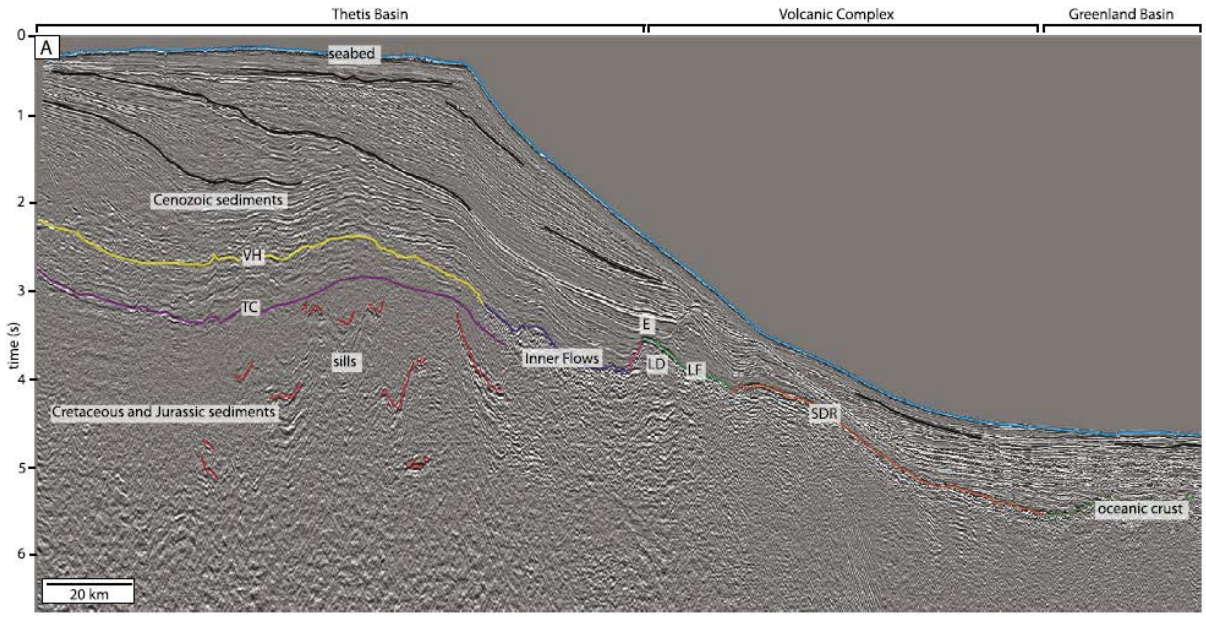

Figure 5. Seismic sections across the Thetis Basin showing the Vent Horizon (VH) terminating against the Inner Flows. SDR=Seaward Dipping Reflection, LF=Landward Flows, LD=Lava Delta, E=Escarpment.

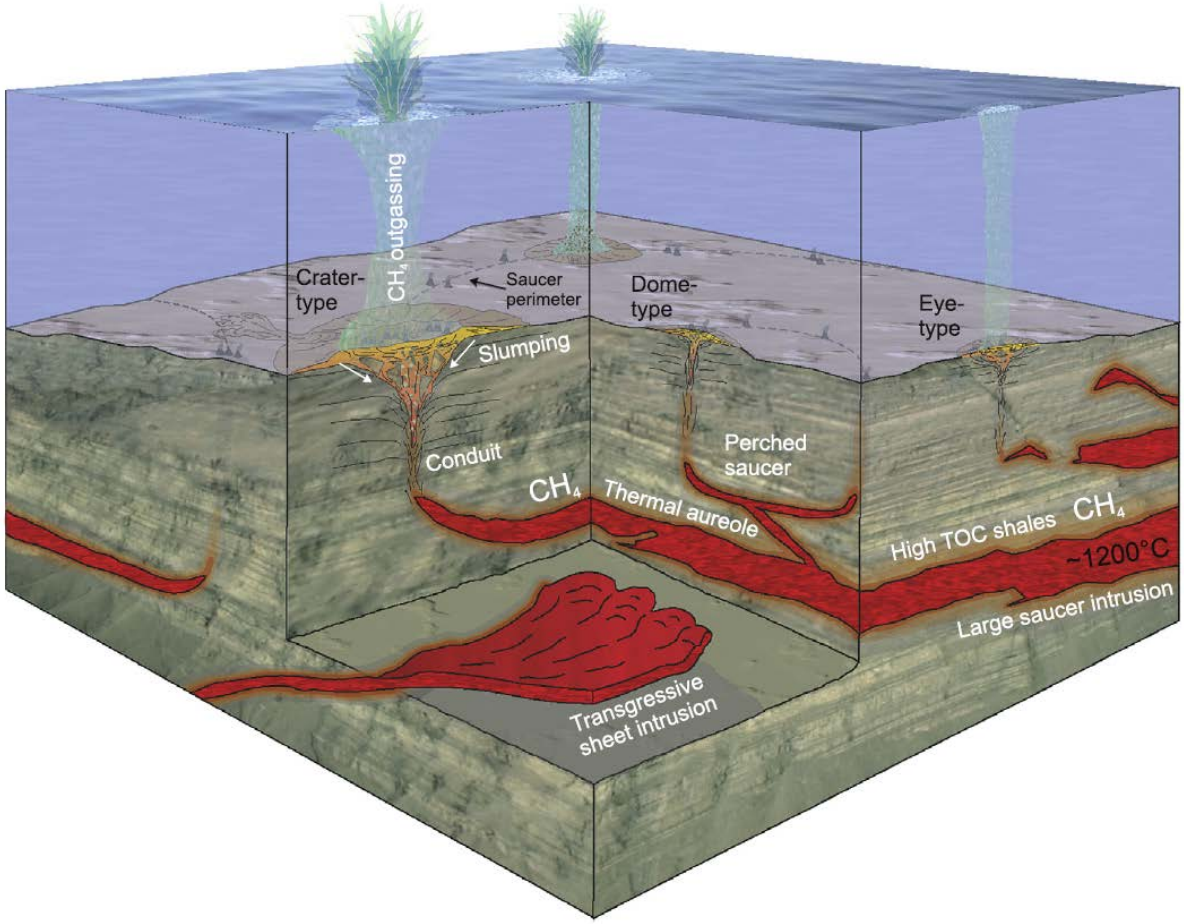

Figure 6. Schematic diagram illustrating the relationship of hydrothermal vents to underlying intrusions, and the subsequent release of CH_4.

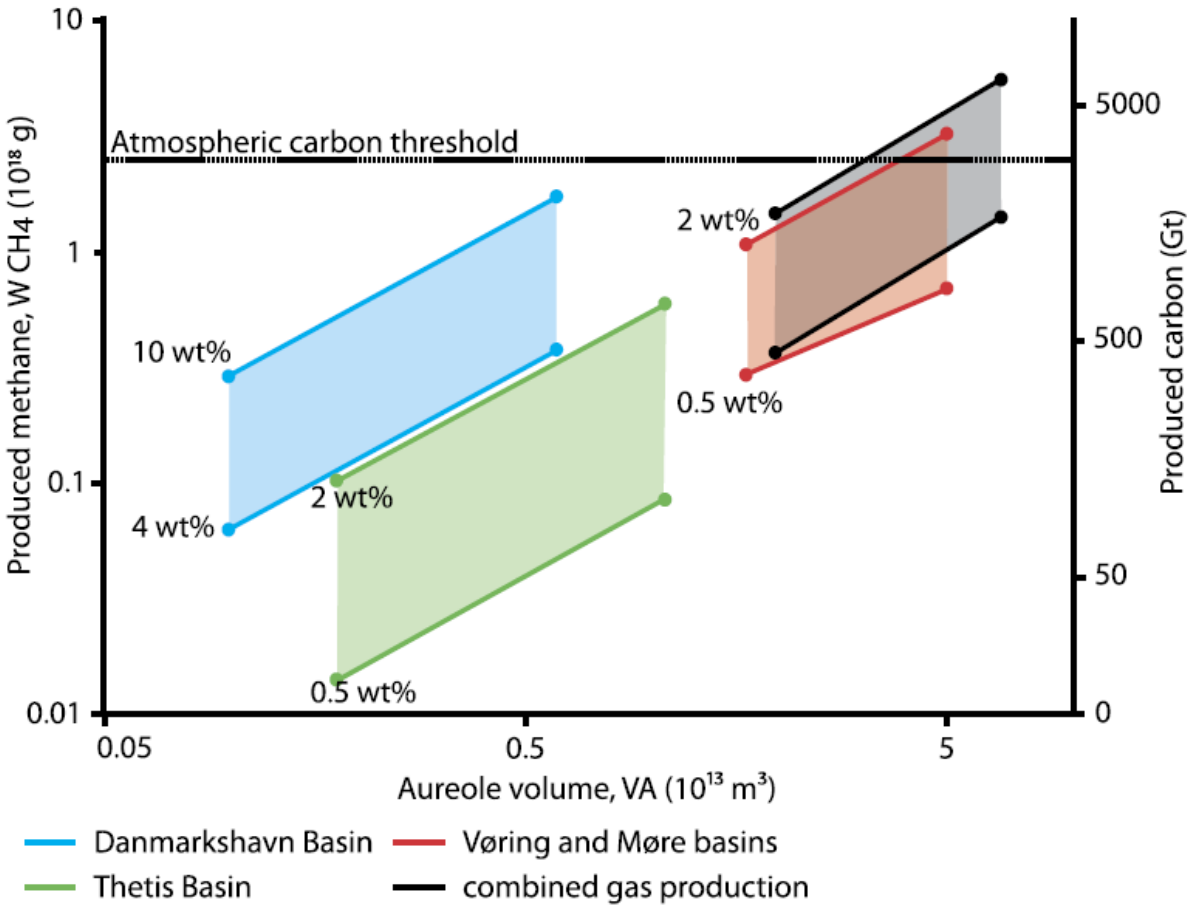

Figure 7. Graph showing estimated gas production from the Danmarkshavn, Thetis and Vøring and Møre basins. The black lines represent the minimum and maximum values for the combined gas production in these basins. The dashed line represents the threshold value of methane required to have produced the negative $\delta^{13}C$ excursion observed during the PETM. Gas production varies as a function of sill complex area, intrusion thickness and the TOC contents (shown in wt %) of the host sedimentary rocks.